Manuscript

Larger but younger fish when growth compensates for higher mortality in heated ecosystem

Max Lindmark[a,b,1], Malin Karlsson[a], Anna Gårdmark[c]

[a] Swedish University of Agricultural Sciences, Department of Aquatic Resources, Institute of Coastal Research, Skolgatan 6, 742 42 Öregrund, Sweden

[b] Swedish University of Agricultural Sciences, Department of Aquatic Resources, Institute of Marine Research, Turistgatan 5, 453 30 Lysekil, Sweden

[c] Swedish University of Agricultural Sciences, Department of Aquatic Resources, Skolgatan 6, SE-742 42 Öregrund, Sweden

[1] Author to whom correspondence should be addressed. Current address:
Max Lindmark, Swedish University of Agricultural Sciences, Department of Aquatic Resources, Institute of Marine Research, Turistgatan 5, 453 30 Lysekil, Sweden, Tel.: +46(0)104784137, email: max.lindmark@slu.se

Keywords: body growth, size-structure, size-spectrum, mortality, climate change

Abstract

Ectotherms are often predicted to "shrink" with global warming, in line with general growth models and the temperature-size rule (TSR), both predicting smaller adult sizes with warming. However, they also predict faster juvenile growth rates, leading to larger size-at-age. Hence, the result of warming on population size-structure also depends on mortality rates and how much also adult size changes. We used data from an artificially heated (+8C) bay in comparison with an unheated area, to analyze how warming has affected body growth, mortality rates and population size-structure of Eurasian perch (*Perca fluviatilis*). In the heated bay, body size was larger for all ages and growth faster for all sizes, resulting in larger size-spectrum exponent (greater proportion of large fish) – despite higher mortality. Hence, to understand how warming alters species size-structure, and thus ecological interactions and dynamics, it is critical to account for warming-induced changes in both mortality and growth rate.

Introduction

Ectotherm species, constituting 99% of species globally[1,2], are commonly predicted to shrink in a warming world[3–5]. Mean body size responses to temperature may however be uninformative, as the size-distribution of many species spans several orders of magnitude. Warming can even shift size-distributions without altering mean size; for example, if increases in juvenile size-at-age outweigh the decline in size-at-age in adults, which is consistent with the temperature size-rule, TSR[6]. Resolving how warming induces changes in population size-distributions may thus be more instructive[7], especially for inferring warming effects on species' ecological role, biomass production, or energy fluxes[8]. This is because key traits such as metabolism, feeding, growth, mortality scale with body size[9–14]. Hence, as the value of these traits at mean body size is not the same as the mean population trait value[15], the size-distribution within a population thus matters for its dynamics under warming,

The population size distribution can be represented as a size-spectrum, which generally is the frequency distribution of individual body sizes[16]. It is often described in terms of the spectrum slope (slope of individuals or biomass of a size class over the mean size of that class on log-log scale[16–18]) or simply the exponent of the power law individual size-distribution[16]. The size-spectrum thus results from temperature-dependent ecological processes such as body growth, mortality and recruitment[10,19]. Despite its rich theoretical foundation[20] and usefulness as an ecological indicator[21], few studies have evaluated warming-effects on the species size-spectrum in larger bodied species (but see Blanchard *et al.*[21]). There are numerous paths by which the species size-spectrum could change with warming[19]. For instance, the clearest consequence of TSR for the size-spectrum is a decline in maximum size. However, unless warming also alters the relative abundances of juveniles and adults, the same number of adults will accumulate in a smaller size-range, resulting in a less steep slope of the size-spectrum. Warming can also lead to elevated mortality, which truncates the age-distribution towards

99 younger individuals[22]. Increased growth rates can however counter the effects of mortality on
100 abundance-at-size, unless only small individuals benefit from warming[23,24]. Growth rates can
101 increase due to physiological responses to higher temperatures, or reduced density-dependence
102 following warming-induced mortality, or both. Hence, the effect of warming on the size-
103 spectrum depends on several interlinked processes affecting abundance-at-size and size-at-age.
104 Yet, while warming effects on ectotherm body growth have been thoroughly studied[6,24,25],
105 those on mortality in wild populations have not to the same extent, nor their joint consequences
106 for population size-spectra in warming environments.
107 We used data from a unique, large-scale 23-year-long heating-experiment of a coastal
108 ecosystem to quantify how warming changed fish body growth, mortality, and the size structure
109 in an unexploited population of Eurasian perch (*Perca fluviatilis*, 'perch'). We compare fish
110 from this enclosed bay exposed to temperatures 5-10 ℃ above normal ('heated area') with fish
111 from a reference area in the adjacent archipelago (Fig. 1). Using hierarchical Bayesian models,
112 we quantify differences in key individual- and population level parameters, such as body
113 growth, asymptotic size, mortality rates, and size-spectra, between the heated and reference
114 coastal area.
115

116 ## Results

117 Analysis of fish (perch) size-at-age using the von Bertalanffy growth equation (VBGE)
118 revealed that fish cohorts (year classes) in the heated area both grew faster initially (larger size-
119 at-age and VBGE K parameter) and reached larger predicted asymptotic sizes than those in the
120 reference area (Fig. 2). The model with area-specific VBGE parameters (L_∞, K and t_0) had
121 best out of sample predictive accuracy (the largest expected log pointwise predictive density
122 for a new observation; Table S1), and there is a clear difference in both the estimated values
123 for fish asymptotic length (L_∞) and growth rate (K) between the heated and reference area (Fig.

2B-E). For instance, the distribution of differences between the heated and reference area of the posterior samples for L_∞ and K only had 11% and 2%, respectively, of the density below 0, illustrating that it is unlikely that the parameters are larger in the reference area or similar in the two areas (Fig. 2C, E). We estimated that fish in the heated area had a 16% larger asymptotic length than in the reference area ($L_{\infty heat} = 45.7[36.8, 56.3]$, $L_{\infty ref} = 39.4[35.4, 43.9]$, given as posterior median with 95% credible interval) and 27% larger growth coefficient ($K_{heat} = 0.19[0.15, 0.23], K_{ref} = 0.15[0.12, 0.17]$). Corresponding estimates of the third parameter in the VBGE were $t_{0heat} = -0.16[-0.21, -0.11]$, and $t_{0ref} = -0.44[-0.56, -0.33]$.

In addition, we found that the initial growth rate (at small size) was higher in the heated area and that the decline in growth with length was steeper in the reference area (Fig. 3). The best model for growth ($G = \alpha L^{\theta}$) had area-specific parameters (Table S2), and we found even stronger support for differences in growth parameters between the areas (Fig. 3). Initial growth was estimated to be 18% faster in the heated than in the reference area ($\alpha_{heat} = 509.7[460.1,563.5]$, $\alpha_{ref} = 433.5[413.3,454.1]$), and growth of fish in the heated area had a 4% lower decline with length than in the reference area ($\theta_{heat} = -1.13[-1.16, -1.11]$, $\theta_{ref} = -1.18[-1.19, -1.16]$). The distribution of differences of the posterior samples for α and θ both only had 0.3% of the density below 0 (Fig. 3C, E), indicating high probability that growth rates have differentiated between the heated and reference area.

By analyzing the decline in catch-per-unit-effort over age, we found that the instantaneous mortality rate Z (rate at which log abundance declines with age) is higher in the heated area (Fig. 4). The overlap with zero is 0.1% for the distribution of differences of posterior samples of Z_{heat} and Z_{ref} (Fig. 4C). We estimated Z_{heat} to be $0.76[0.63,0.88]$ and Z_{ref} to be $0.63[0.58,0.69]$, which corresponds to annual mortality rates of 53% in the heated area and 47% in the reference area.

149 Lastly, analysis of the size-structure in the two areas revealed that the faster growth rates
150 for fish of all sizes, which lead to a larger size-at-age, outweigh the higher mortality rates in
151 the heated area, such that the size-spectrum exponent is larger in the heated area (Fig. 5A).
152 However, in contrast to the results on size-at-age, growth and mortality, the differentiation is
153 not as strong statistically, as the 95% confidence intervals overlap. That said, because of this
154 faster growth, the heated area both has the largest individuals and an overall larger proportion
155 of large individuals (Fig. 5C).
156

157 ## Discussion

158 Our study provides strong evidence for warming-induced differentiation in growth, mortality,
159 and size-structure in a natural population of an unexploited, temperate fish species exposed to
160 5-10 ℃ above normal temperatures for more than two decades. While it is a study on only a
161 single species, these features make it a unique climate change experiment, as experimental
162 studies on fish to date are much shorter and long time series exist mainly for commercially
163 exploited fish species (and fisheries exploitation affects size-structure both directly and
164 indirectly by selecting for fast growing individuals)[26]. While factors other than temperature
165 could have contributed to the elevated growth and mortality, the temperature contrast is
166 unusually large for natural systems (i.e., 5-10 ℃, which can be compared to the 1.35 ℃ change
167 in the Baltic Sea between 1982 and 2006[27]). Moreover, heating occurred at the scale of a whole
168 ecosystem, which makes the findings highly relevant in the context of global warming.
169 Interestingly, our findings contrast with both broader predictions about declining mean or
170 adult body sizes based on the GOLT hypothesis[5,28], and with intraspecific patterns such as the
171 TSR (temperature-size rule; Atkinson[6]). The contrasts lie in that both asymptotic size and size-
172 at-age of mature individuals, as well as the proportion of larger individuals were larger and
173 higher in the heated area—despite the elevated mortality rates. Since optimum growth

174 temperatures decline with size within species generally under food satiation in experimental
175 studies[24], the finding that the largest asymptotic size and the largest individuals were found in
176 the heated area was unexpected. This suggests that growth dynamics under food satiation may
177 not be directly proportional to those under natural feeding conditions[29]. Our results suggest that
178 growth changes emerge not only from direct physiological responses to increased temperatures,
179 but also from warming-induced changes in the food web, e.g., prey productivity, diet
180 composition and trophic transfer efficiencies[30]. Moreover, it also highlights that we need to
181 focus on gaining understanding to what extent the larger size-at-age for juveniles in warm
182 environments that is commonly observed can be maintained as they grow older.

183 Our finding that mortality rates were higher in the heated area was expected—warming
184 leads to faster metabolic rates, which in turn is associated with shorter life span[11,31,32] (higher
185 "physiological" mortality). Warming may also increase predation mortality, as predators'
186 feeding rates increase in order to meet the higher demand of food[12,14,33]. However, most
187 evidence to date of the temperature dependence of mortality rates in natural populations stem
188 from across species studies[12,13,34] (but see[33,35]). Across species relationships are not necessarily
189 determined by the same processes as within species relationships; thus our finding of warming-
190 induced mortality in a heated vs control environment in two nearby con-specific populations is
191 important. Since a key question for understanding the implications of warming on ectotherm
192 populations is if larger individuals in a population become rarer or smaller[36,37], within-species
193 mortality responses to warming need further study. Importantly, this requires accounting also
194 for effects of warming on growth, and how responses in growth and mortality depend on each
195 other. For instance, higher mortality (predation or natural, physiological mortality) can release
196 intra-specific competition and thus increase growth. Conversely, altered growth and body sizes
197 can lead to changes in size-specific mortality, such as predation or starvation. In conclusion,
198 understanding how the size- and age-distribution change rather than the mean size is critical

for predicting how warming changes species functions and ecological roles[7,30,38]. Key to do this is to acknowledge temperature effects on both growth and mortality and how they interact.

Materials and Methods

Data

We use size-at-age data from perch sampled annually from the heated enclosed bay ('the Biotest lake') and its reference area with natural temperatures in the years after the onset of warming (first cohort is 1981, and first and last catch year is 1987 and 2003, respectively) to omit transient dynamics and acute responses, and to ensure we use cohorts that only experienced one of the thermal environments during its life. A grid at the outlet of the heated area (Fig. 1) prevented fish larger than 10 cm from migrating between the areas[39,40], and genetic studies confirm the reproductive isolation between the two populations during this time-period[41]. However, since the grid removal in 2004, fish growing up in the heated Biotest lake can easily swim out, meaning we cannot be sure fish in the reference area did not recently arrive from the Biotest lake. Hence, we use data up until 2003. This resulted in 12658 length-at-age measurements from 2426 individuals in 256 net deployments.

We use data from fishing events using survey-gillnets that took place in October in the heated Biotest lake and in August in the reference area when temperatures are most comparable between the two areas[40], because temperature affect catchability in static gears. The catch was recorded by 2.5 cm length classes during 1987-2000, and into 1 cm length groups between 2001-2003. To express lengths in a common length standard, 1 cm intervals were converted into 2.5 cm intervals. The unit of catch data is hence the number of fish caught per 2.5 cm size class per night per net (i.e., a catch-per-unit-effort [CPUE] variable). All data from fishing events with disturbance affecting the catch (e.g., seal damage, strong algal growth on the gears,

223 clogging by drifting algae) were removed (years 1996 and 1999 from the heated area in the
224 catch data).

225 Length-at-age was reconstructed for a semi-random length-stratified subset of individuals
226 each year. This was done using annuli rings on the operculum bones (with control counts done
227 on otoliths), and an established power-law relationship between the distance of annual rings
228 and fish length: $L = \kappa R^s$, where L is the length of the fish, R the operculum radius, κ the
229 intercept, and s the slope of the line for the regression of log-fish length on log-operculum
230 radius from a large reference data set for perch[42]. Back-calculated length-at-age were obtained
231 from the relationship $L_a = L_s(\frac{r_a}{R})^s$, where L_a is the back-calculated body length at age a, L_s
232 is the final body length (body length at catch), r_a is the distance from the center to the annual
233 ring corresponding to age a and $s = 0.861$ for perch[42]. Since perch exhibits sexual size-
234 dimorphism, and age-determination together with back calculation of growth was not done for
235 males in all years, we only used females for our analyses.

236

237 *Statistical Analysis*

238 The differences in size-at-age, growth, mortality, and size structure between the heated and the
239 reference area were quantified using hierarchical linear and non-linear regression models fitted
240 in a Bayesian framework. First, we describe each statistical model and then provide details of
241 model fitting, model diagnostics and comparison.

242 We fit the von Bertalanffy growth equation (VBGE) on a log scale, describing length as a
243 function of age to evaluate differences in size-at-age and asymptotic size: $log\,(L_t) =$
244 $log\,(L_\infty(1 - e^{(-K(t-t_0))}))$, where L_t is the length at age (t, years), L_∞ is the asymptotic size,
245 K is the Brody coefficient (yr^{-1}) and t_0 is the age when the average length was zero. We used
246 only age- and size-at-catch as the response variables (i.e., not back-calculated length-at-age).
247 This was to have a simpler model and not have to account for parameters varying within

individuals as well as cohorts, as mean sample size per individual was only ~5. We let parameters vary among cohorts rather than year of catch, because individuals within cohorts share similar environmental conditions and density dependence[43]. Eight models in total were fitted (with area being dummy-coded), with different combinations of shared and area-specific parameters. We evaluated if models with area-specific parameters led to better fit and quantified the differences in area-specific parameters. The model with all area-specific parameter can be written as:

$$L_i \sim \text{Student-}t(\upsilon, \mu_i, \sigma) \tag{1}$$

$$\log(\mu_i) = A_R \log\left[L_{\infty Rj[i]}\left(1 - e^{\left(-K_{Rj[i]}\left(t - t_{0Rj[i]}\right)\right)}\right)\right] + A_H \log\left[L_{\infty Hj[i]}\left(1 - e^{\left(-K_{Hj[i]}\left(t - t_{0Hj[i]}\right)\right)}\right)\right] \tag{2}$$

$$\begin{bmatrix} L_{\infty Rj} \\ L_{\infty Hj} \\ K_{Rj} \\ K_{Hj} \end{bmatrix} \sim \text{MVNormal}\left(\begin{bmatrix} \mu_{L_{\infty R}} \\ \mu_{L_{\infty H}} \\ \mu_{K_R} \\ \mu_{K_H} \end{bmatrix}, \begin{bmatrix} \sigma_{L_{\infty R}} & 0 & 0 & 0 \\ 0 & \sigma_{L_{\infty H}} & 0 & 0 \\ 0 & 0 & \sigma_{K_R} & 0 \\ 0 & 0 & 0 & \sigma_{K_H} \end{bmatrix}\right) \tag{3}$$

where lengths are $Student - t$ distributed to account for extreme observations, υ, μ and ϕ represent the degrees of freedom, mean and the scale parameter, respectively. Henceforth, subscripts H and R are used for the heated and reference area, respectively (except in figures and main text where subscripts are spelled out for clarity). A_R and A_H are dummy variables such that $A_R = 1$ and $A_H = 0$ if it is the reference area, and vice versa. The multivariate normal distribution in Eq. 3 is the prior for the cohort-varying parameters $L_{\infty Rj}$, $L_{\infty Hj}$, K_{Rj} and K_{Hj} (for cohorts $j = 1981,\ldots,1997$) (note that cohorts extend further back in time than the catch data), with hyper-parameters $\mu_{L_{\infty R}}$, $\mu_{L_{\infty H}}$, μ_{K_R}, μ_{K_H} describing the non-varying population means and a covariance matrix with the between-cohort variation along the diagonal (note we did not model a correlation between the parameters, hence off-diagonals are 0). The other seven models include some or all parameters as parameters common for the two areas, e.g., substituting $L_{\infty Rj}$ and $L_{\infty Hj}$ with $L_{\infty j}$. To aid convergence of this non-linear model, we used

informative priors chosen after visualizing draws from prior predictive distributions[44] using probable parameter values (*Supporting Information*, Fig. S1, S7). We used the same prior distribution for each parameter class for both areas to not introduce any other sources of differences in parameter estimates between areas. We used the following priors for the VBGE model: $\mu_{L_{\infty R,H}} \sim N(45,20)$, $\mu_{K_{R,H}} \sim N(0.2, 0.1)$, $t_{0R,H} \sim N(-0.5, 1)$ and $\upsilon \sim gamma(2,0.1)$. σ, $\mu_{L_{\infty R}}, \mu_{L_{\infty H}}, \mu_{K_R}, \mu_{K_H}$ were given a $Student - t(3,0,2.5)$ prior.

We also compared how growth scales with body size (in contrast to length vs age) in the two areas, by fitting allometric growth models describing how specific growth rate scales with length: $G = \alpha L^{\theta}$, where G, the specific growth, is defined as: $G = 100 \times (log\ (L_2) - log\ (L_1))/(t_2 - t_1)$ and L is the geometric mean length: $L = (L_1 \times L_2)^{0.5}$. Here we also used back-calculated length-at-age, resulting in multiple observations for each individual. As with the VBGE model, we dummy coded area to compare models with different combinations of common and shared parameters. We assumed growth rates were $Student - t$ distributed, and the full model can be written as:

$$L_i \sim Student - t(\upsilon, \mu_i, \sigma) \quad (4)$$

$$\mu_i = A_R\left(\alpha_{Rj[i],k[i]} L^{\theta_R}\right) + A_H\left(\alpha_{Hj[i],k[i]} L^{\theta_H}\right) \quad (5)$$

$$\alpha_{R,Hj} \sim N\left(\mu_{\alpha_{R,Hj}}, \sigma_{\alpha_{R,Hj}}\right) \quad (6)$$

$$\alpha_{R,Hj} \sim N\left(\mu_{\alpha_{R,Hj}}, \sigma_{\alpha_{R,Hj}}\right) \quad (7)$$

$$\theta_{R,Hj} \sim N\left(\mu_{\theta_{R,Hj}}, \sigma_{\theta_{R,Hj}}\right) \quad (8)$$

$$\theta_{R,Hj} \sim N\left(\mu_{\theta_{R,Hj}}, \sigma_{\theta_{R,Hj}}\right) \quad (9)$$

We assumed only α varied across individuals j within cohorts k and compared two models: one with θ common for the heated and reference area, and one with an area-specific θ. We used the following priors, after visual exploration of the prior predictive distribution (*Supporting Information*, Fig. S7, S9): $\alpha_{R,H} \sim N(500, 100)$, $\theta_{R,H} \sim N(-1.2, 0.3)$ and $\upsilon \sim gamma(2,0.1)$. σ, $\sigma_{id:cohort}$ and σ_{cohort} were all given a $Student - t(3,0,13.3)$ prior.

We estimated total mortality by fitting linear models to the natural log of catch (CPUE) as a function of age (catch curve regression), under the assumption that in a closed population, the exponential decline can be described as $N_t = N_0 e^{-Zt}$, where N_t is the population at time t, N_0 is the initial population size and Z is the instantaneous mortality rate. This equation can be rewritten as a linear equation: $log\ (C_t)\ = log\ (vN_0)\ - Zt$, where C_t is catch-at-age t, if catch is assumed proportional to the number of fish (i.e., $C_t = vN_t$). Hence, the negative of the slope of the regression is Z. To get catch-at-age data, we constructed area-specific age-length keys using the sub-sample of the total catch that was age-determined. Age length-keys describe the age-proportions of each length-category (i.e., a matrix with length category as rows, ages as columns). Age composition is then estimated for the total catch based on the "probability" of fish in each length-category being a certain age. With fit this model with and without an age-$area$-interaction, and the former can be written as:

$$\log\,(CPUE_i) \sim \text{Student-}t(v, \mu_i, \sigma) \tag{10}$$

$$\mu_i = \beta_{0j[i]}(area_R) + \beta_{1j[i]}(area_H) + \beta_{2j[i]} age + \beta_{3j[i]}(age \times area_H) \tag{11}$$

$$\begin{bmatrix}\beta_{0j}\\ \beta_{1j}\\ \beta_{2j}\\ \beta_{3j}\end{bmatrix} \sim \text{MVNormal}\left(\begin{bmatrix}\mu_{\beta_0}\\ \mu_{\beta_1}\\ \mu_{\beta_2}\\ \mu_{\beta_3}\end{bmatrix}, \begin{bmatrix}\sigma_{\beta_0} & 0 & 0 & 0\\ 0 & \sigma_{\beta_1} & 0 & 0\\ 0 & 0 & \sigma_{\beta_2} & 0\\ 0 & 0 & 0 & \sigma_{\beta_3}\end{bmatrix}\right) \tag{12}$$

where β_{0j} and β_{1j} are the intercepts for the reference and heated areas, respectively, β_{2j} is the age slope for the reference area and β_{3j} is the interaction between age and $area$. All parameters vary by cohort (for cohort $j = 1981, \ldots, 2000$) and their correlation is set to 0 (Eq. 12). We use the following (vague) priors: $\mu_{\beta_{0,\ldots,3j}} \sim N(0, 10)$ (where μ_{β_2} is the population-level estimate for $-Z_R$ and $\mu_{\beta_2} + \mu_{\beta_3}$ is the population-level estimate for $-Z_H$) and $v \sim gamma(2, 0.1)$. σ and $\sigma_{\beta_{0,\ldots,3}}$ were given a $Student - t(3, 0, 2.5)$ prior.

Lastly, we quantified differences in the size-distributions between the areas using size-spectrum exponents. We estimate the biomass size-spectrum exponent γ directly, using the

likelihood approach for binned data, i.e., the *MLEbin* method in the R package *sizeSpectra*[16,45,46]. This method explicitly accounts for uncertainty in body masses *within* size-classes (bins) in the data and has been shown to be less biased than regression-based methods or the likelihood method based on bin-midpoints[16,45]. We pooled all years to ensure negative relationships between biomass and size in the size-classes (as the sign of the relationship varied between years).

All analyses were done using R[47] version 4.0.2 with R Studio (2021.09.1). The packages within the *tidyverse*[48] collection were used to processes and visualize data. Models where fit using the R package *brms*[49]. When priors were not chosen based on the prior predictive distributions, we used the default priors from *brms* as written above. We used 3 chains and 4000 iterations in total per chain. Models were compared by evaluating their expected predictive accuracy (expected log pointwise predictive density) using leave-one-out cross-validation (LOO-CV)[50] while ensuring pareto k values < 0.7, in the R package *loo*[51]. Results of the model comparison can be found in the *Supporting Information*, Table S1-S4. We used *bayesplot*[52] and *tidybayes*[53] to process and visualize model diagnostics and posteriors. Model convergence and fit was assessed by ensuring potential scale reduction factors ($\hat{R}$) were less than 1.1, suggesting all three chains converged to a common distribution)[54], and by visually inspecting trace plots, residuals QQ-plots and with posterior predictive checks (*Supporting Information*, Fig. S2, S8, S10).

Acknowledgements

We thank all staff involved in data collection. This study was supported by SLU Quantitative Fish and Fisheries Ecology.

Code and Data Availability

All data and R code to reproduce the analyses can be downloaded from a GitHub repository (https://github.com/maxlindmark/warm_life_history) and will be archived on Zenodo upon publication.

Author Contributions

ML conceived the idea and designed the study and the statistical analysis. Data-processing, initial statistical analyses, and initial writing was done by MK and ML. AG contributed critically to all mentioned parts of the paper. All authors contributed to the manuscript writing and gave final approval for publication.

References

1. Wilson, E. O. *The Diversity of Life*. (Harvard University Press, 1992).
2. Atkinson, D. & Sibly, R. M. Why are organisms usually bigger in colder environments? Making sense of a life history puzzle. *Trends in Ecology & Evolution* **12**, 235–239 (1997).
3. Gardner, J. L., Peters, A., Kearney, M. R., Joseph, L. & Heinsohn, R. Declining body size: a third universal response to warming? *Trends in Ecology & Evolution* **26**, 285–291 (2011).
4. Sheridan, J. A. & Bickford, D. Shrinking body size as an ecological response to climate change. *Nature Climate Change* **1**, 401–406 (2011).
5. Cheung, W. W. L. *et al.* Shrinking of fishes exacerbates impacts of global ocean changes on marine ecosystems. *Nature Climate Change* **3**, 254–258 (2013).
6. Atkinson, D. Temperature and organism size—A biological law for ectotherms? in *Advances in Ecological Research* vol. 25 1–58 (Elsevier, 1994).

7. Fritschie, K. J. & Olden, J. D. Disentangling the influences of mean body size and size structure on ecosystem functioning: an example of nutrient recycling by a non-native crayfish. *Ecology and Evolution* **6**, 159–169 (2016).
8. Yvon-Durocher, G., Montoya, J. M., Trimmer, M. & Woodward, G. Warming alters the size spectrum and shifts the distribution of biomass in freshwater ecosystems. *Global Change Biology* **17**, 1681–1694 (2011).
9. Andersen, K. H. Size-based theory for fisheries advice. *ICES J Mar Sci* **77**, 2445–2455 (2020).
10. Blanchard, J. L., Heneghan, R. F., Everett, J. D., Trebilco, R. & Richardson, A. J. From bacteria to whales: Using functional size spectra to model marine ecosystems. *Trends in Ecology & Evolution* **32**, 174–186 (2017).
11. Brown, J. H., Gillooly, J. F., Allen, A. P., Savage, V. M. & West, G. B. Toward a metabolic theory of ecology. *Ecology* **85**, 1771–1789 (2004).
12. Pauly, D. On the interrelationships between natural mortality, growth parameters, and mean environmental temperature in 175 fish stocks. *ICES Journal of Marine Science* **39**, 175–192 (1980).
13. Thorson, J. T., Munch, S. B., Cope, J. M. & Gao, J. Predicting life history parameters for all fishes worldwide. *Ecological Applications* **27**, 2262–2276 (2017).
14. Ursin, E. A Mathematical Model of Some Aspects of Fish Growth, Respiration, and Mortality. *Journal of the Fisheries Research Board of Canada* **24**, 2355–2453 (1967).
15. Bernhardt, J. R., Sunday, J. M., Thompson, P. L. & O'Connor, M. I. Nonlinear averaging of thermal experience predicts population growth rates in a thermally variable environment. *Proceedings of the Royal Society B: Biological Sciences* **285**, 20181076 (2018).

16. Edwards, A. M., Robinson, J. P. W., Plank, M. J., Baum, J. K. & Blanchard, J. L. Testing and recommending methods for fitting size spectra to data. *Methods in Ecology and Evolution* **8**, 57–67 (2017).
17. Sheldon, R. W., Sutcliffe, W. H. & Prakash, A. The Production of Particles in the Surface Waters of the Ocean with Particular Reference to the Sargasso Sea1. *Limnology and Oceanography* **18**, 719–733 (1973).
18. White, E. P., Ernest, S. K. M., Kerkhoff, A. J. & Enquist, B. J. Relationships between body size and abundance in ecology. *Trends in Ecology & Evolution* **22**, 323–330 (2007).
19. Heneghan, R. F., Hatton, I. A. & Galbraith, E. D. Climate change impacts on marine ecosystems through the lens of the size spectrum. *Emerging Topics in Life Sciences* **3**, 233–243 (2019).
20. Andersen, K. H. *Fish Ecology, Evolution, and Exploitation: A New Theoretical Synthesis*. (Princeton University Press, 2019).
21. Blanchard, J. L. *et al.* Do climate and fishing influence size-based indicators of Celtic Sea fish community structure? *ICES Journal of Marine Science* **62**, 405–411 (2005).
22. Barnett, L. A. K., Branch, T. A., Ranasinghe, R. A. & Essington, T. E. Old-Growth Fishes Become Scarce under Fishing. *Current Biology* **27**, 2843-2848.e2 (2017).
23. Daufresne, M., Lengfellner, K. & Sommer, U. Global warming benefits the small in aquatic ecosystems. *Proceedings of the National Academy of Sciences, USA* **106**, 12788–12793 (2009).
24. Lindmark, M., Ohlberger, J. & Gårdmark, A. Optimum growth temperature declines with body size within fish species. *Global Change Biology* **28**, 2259–2271 (2022).
25. Brett, J. R., Shelbourn, J. E. & Shoop, C. T. Growth rate and body composition of fingerling sockeye salmon, *Oncorhynchus nerka*, in relation to temperature and ration size. *J. Fish. Res. Bd. Can.* **26**, 2363–2394 (1969).

418 26. Baudron, A. R., Needle, C. L., Rijnsdorp, A. D. & Marshall, C. T. Warming temperatures
419 and smaller body sizes: synchronous changes in growth of North Sea fishes. *Global*
420 *Change Biology* **20**, 1023–1031 (2014).
421 27. Belkin, I. M. Rapid warming of large marine ecosystems. *Progress in Oceanography* **81**,
422 207–213 (2009).
423 28. Pauly, D. The gill-oxygen limitation theory (GOLT) and its critics. *Science Advances* **7**,
424 eabc6050 (2021).
425 29. Railsback, S. F. What We Don't Know About the Effects of Temperature on Salmonid
426 Growth. *Transactions of the American Fisheries Society* **151**, 3–12 (2022).
427 30. Gårdmark, A. & Huss, M. Individual variation and interactions explain food web
428 responses to global warming. *Philosophical Transactions of the Royal Society B:*
429 *Biological Sciences* **375**, 20190449 (2020).
430 31. McCoy, M. W. & Gillooly, J. F. Predicting natural mortality rates of plants and animals.
431 *Ecology Letters* **11**, 710–716 (2008).
432 32. Munch, S. B. & Salinas, S. Latitudinal variation in lifespan within species is explained by
433 the metabolic theory of ecology. *Proceedings of the National Academy of Sciences* **106**,
434 13860–13864 (2009).
435 33. Biro, P. A., Post, J. R. & Booth, D. J. Mechanisms for climate-induced mortality of fish
436 populations in whole-lake experiments. *Proceedings of the National Academy of Sciences*
437 **104**, 9715–9719 (2007).
438 34. Gislason, H., Daan, N., Rice, J. C. & Pope, J. G. Size, growth, temperature and the
439 natural mortality of marine fish: Natural mortality and size. *Fish and Fisheries* **11**, 149–
440 158 (2010).

35. Berggren, T., Bergström, U., Sundblad, G. & Östman, Ö. Warmer water increases early body growth of northern pike (Esox lucius) but mortality has larger impact on decreasing body sizes. *Can. J. Fish. Aquat. Sci.* (2021) doi:10.1139/cjfas-2020-0386.
36. Ohlberger, J. Climate warming and ectotherm body size – from individual physiology to community ecology. *Functional Ecology* **27**, 991–1001 (2013).
37. Ohlberger, J., Ward, E. J., Schindler, D. E. & Lewis, B. Demographic changes in Chinook salmon across the Northeast Pacific Ocean. *Fish and Fisheries* **19**, 533–546 (2018).
38. Audzijonyte, A. *et al.* Fish body sizes change with temperature but not all species shrink with warming. *Nat Ecol Evol* **4**, 809–814 (2020).
39. Adill, A., Mo, K., Sevastik, A., Olsson, J. & Bergström, L. *Biologisk recipientkontroll vid Forsmarks kärnkraftverk (in Swedish)*. https://pub.epsilon.slu.se/11349/ (2013).
40. Huss, M., Lindmark, M., Jacobson, P., van Dorst, R. M. & Gårdmark, A. Experimental evidence of gradual size-dependent shifts in body size and growth of fish in response to warming. *Glob Change Biol* **25**, 2285–2295 (2019).
41. Björklund, M., Aho, T. & Behrmann-Godel, J. Isolation over 35 years in a heated biotest basin causes selection on MHC class IIß genes in the European perch (Perca fluviatilis L.). *Ecol Evol* **5**, 1440–1455 (2015).
42. Thoresson, G. *Metoder för övervakning av kustfiskbestånd (in Swedish)*. http://urn.kb.se/resolve?urn=urn:nbn:se:havochvatten:diva-317 (1996).
43. Morrongiello, J. R. & Thresher, R. E. A statistical framework to explore ontogenetic growth variation among individuals and populations: a marine fish example. *Ecological Monographs* **85**, 93–115 (2015).
44. Wesner, J. S. & Pomeranz, J. P. F. Choosing priors in Bayesian ecological models by simulating from the prior predictive distribution. *Ecosphere* **12**, e03739 (2021).

45. Edwards, A. M., Robinson, J. P. W., Blanchard, J. L., Baum, J. K. & Plank, M. J. Accounting for the bin structure of data removes bias when fitting size spectra. *Marine Ecology Progress Series* **636**, 19–33 (2020).
46. Edwards, A. *sizeSpectra: Fitting Size Spectra to Ecological Data Using Maximum Likelihood*. (2020).
47. R Core Team. *R: A Language and Environment for Statistical Computing. R Foundation for Statistical Computing*. (2020).
48. Wickham, H. *et al.* Welcome to the tidyverse. *Journal of Open Source Software* 1686 (2019) doi:https://doi.org/10.21105/joss.01686.
49. Bürkner, P.-C. **brms** : An *R* Package for Bayesian Multilevel Models Using *Stan*. *Journal of Statistical Software* **80**, (2017).
50. Vehtari, A., Gelman, A. & Gabry, J. Practical Bayesian model evaluation using leave-one-out cross-validation and WAIC. *Stat Comput* **27**, 1413–1432 (2017).
51. Vehtari, A. *et al. loo: Efficient leave-one-out cross-validation and WAIC for Bayesian models.* (2020).
52. Gabry, J., Simpson, D., Vehtari, A., Betancourt, M. & Gelman, A. Visualization in Bayesian workflow. *J. R. Stat. Soc. A* **182**, 389–402 (2019).
53. Kay, M. *tidybayes: Tidy Data and Geoms for Bayesian Models*. (2019).
54. Gelman, A., Carlin, J., Stern, H. & Rubin, D. *Bayesian Data Analysis. 2nd edition*. (Chapman and Hall/CRC, 2003).

488 Figures

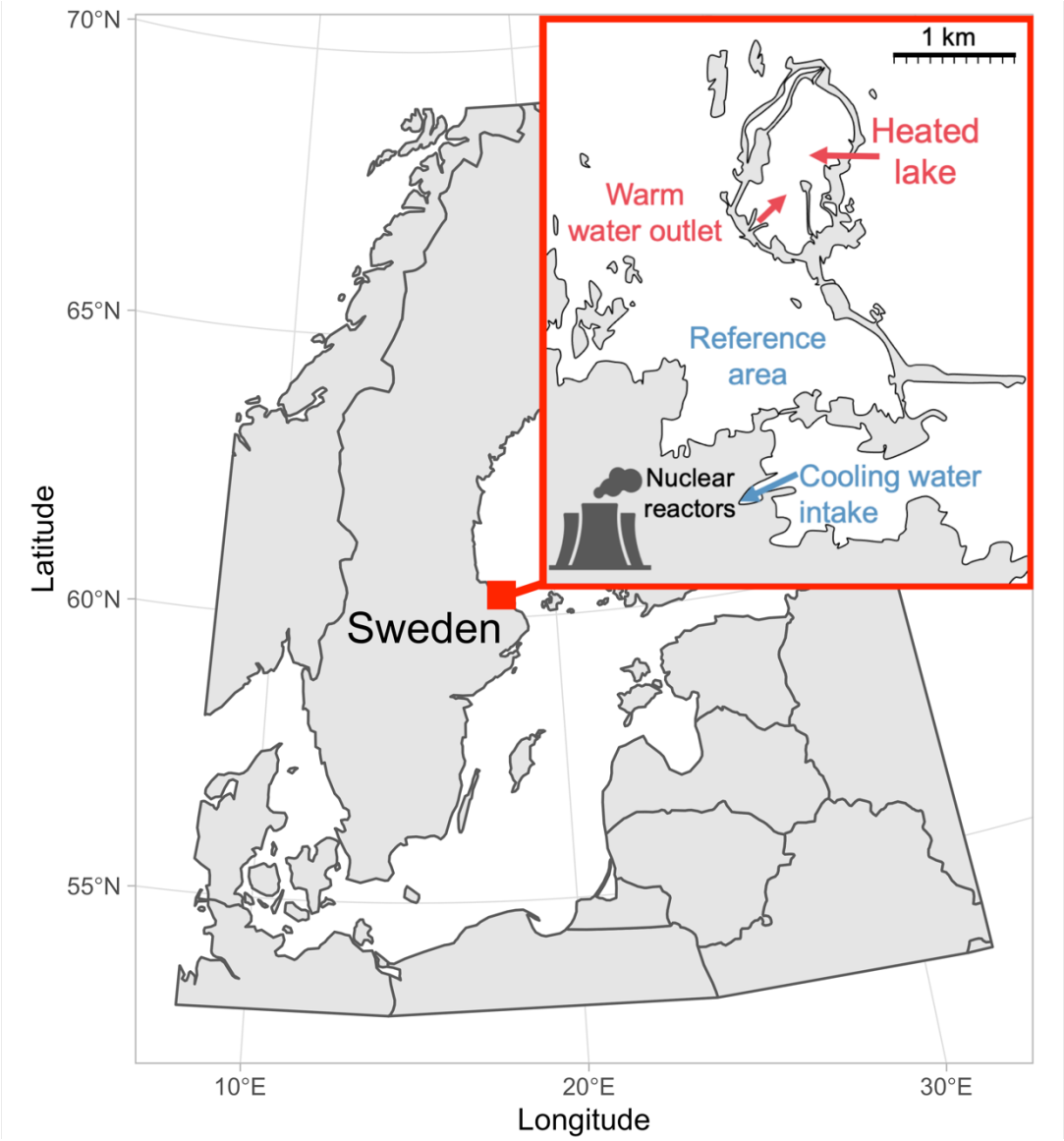

489

490 **Fig. 1.** Map of the area with the unique whole-ecosystem warming experiment from which
491 perch in this study was sampled. Inset shows the 1 km^2 enclosed coastal bay that has been
492 artificially heated for 23 years, the adjacent reference area with natural temperatures, and
493 locations of the cooling water intake and where the heated water outlet from nuclear power
494 plants enters the heated coastal area.

495

496

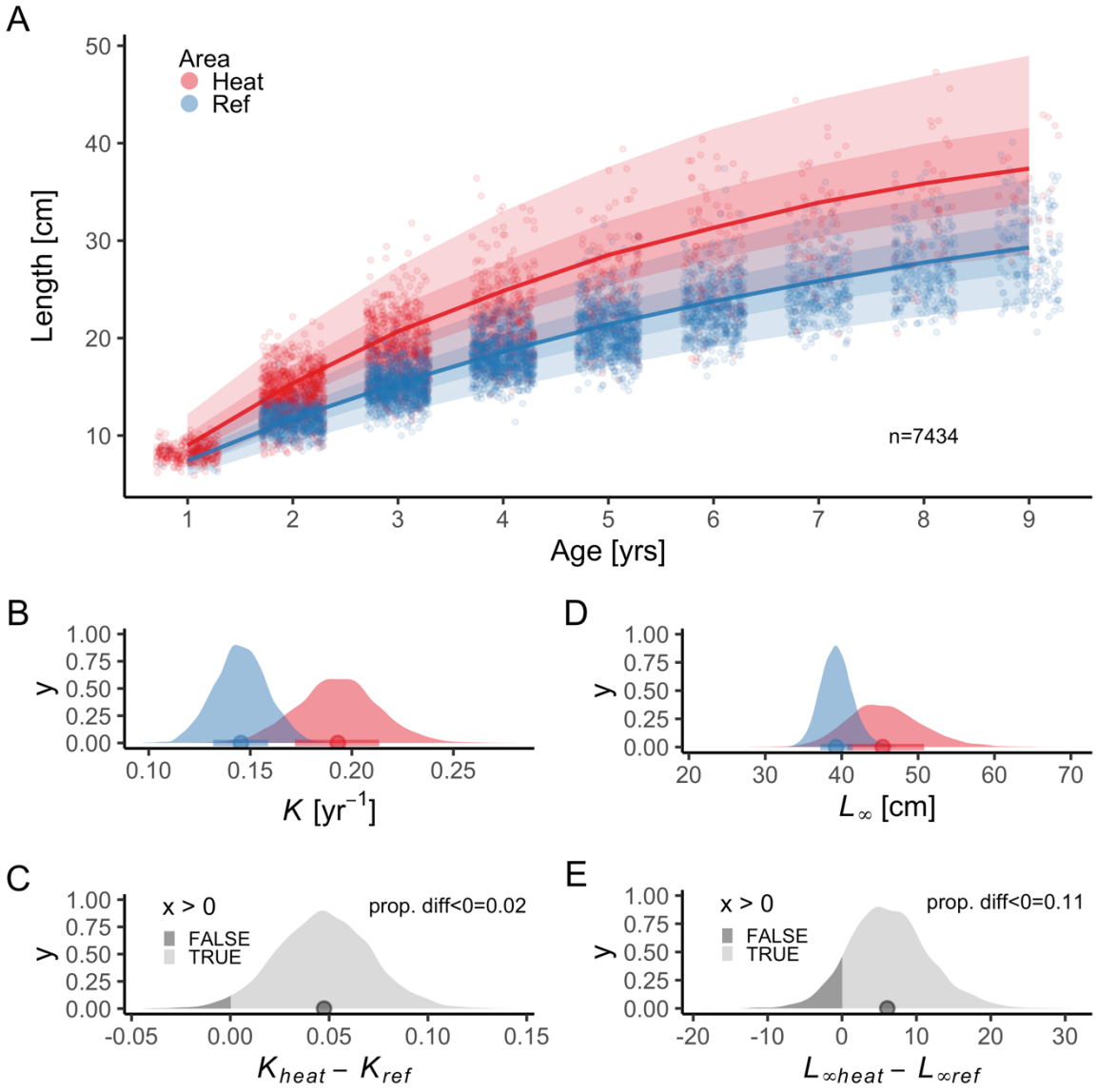

497

498 **Fig. 2.** The average length-at-age is larger for fish of all ages in the heated (red) compared to
499 the reference (blue) coastal area. Points in panel (A) depict individual-level length-at-age and
500 lines show the global posterior prediction (both exponentiated) without group-level effects (i.e.,
501 cohort) from the von Bertalanffy growth model with area-specific coefficients. The shaded
502 areas correspond to 50% and 90% credible intervals. Panel (B) shows the posterior distributions
503 for growth coefficient (parameters K_{heat} (red) and K_{ref} (blue)) and (C) the distribution of their
504 difference. Panel (D) shows the posterior distributions for asymptotic length (parameters
505 $L_{\infty heat}$ and $L_{\infty ref}$), and (E) the distribution of their difference.

506

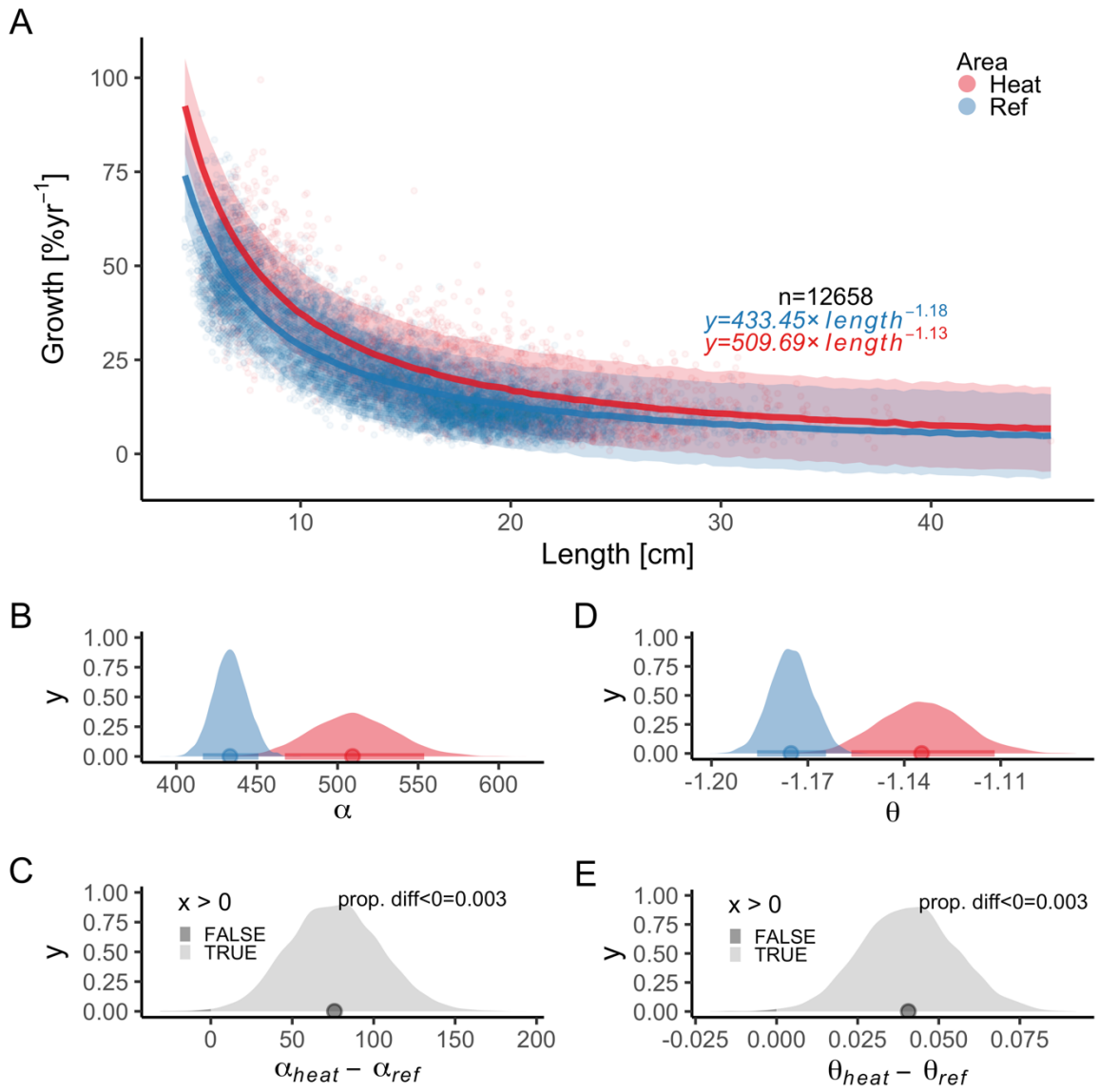

Fig. 3. The faster growth rates in the heated area (red) compared to the reference (blue) are maintained as fish grow. The points illustrate specific growth estimated from back-calculated length-at-age (within individuals) as a function of length (expressed as the geometric mean of the length at the start and end of the time interval). Lines show the global posterior prediction without group-level effects (i.e., individual within cohort) from the allometric growth model with area-specific coefficients. The shaded areas correspond to the 90% credible interval. The equation uses mean parameter estimates. Panel (B) shows the posterior distributions for initial growth (α_{heat} (red) and α_{ref} (blue)), and (C) the distribution of their difference. Panel (D) shows the posterior distributions for the allometric decline in growth with length (θ_{heat} and θ_{ref}), and (E) the distribution of their difference.

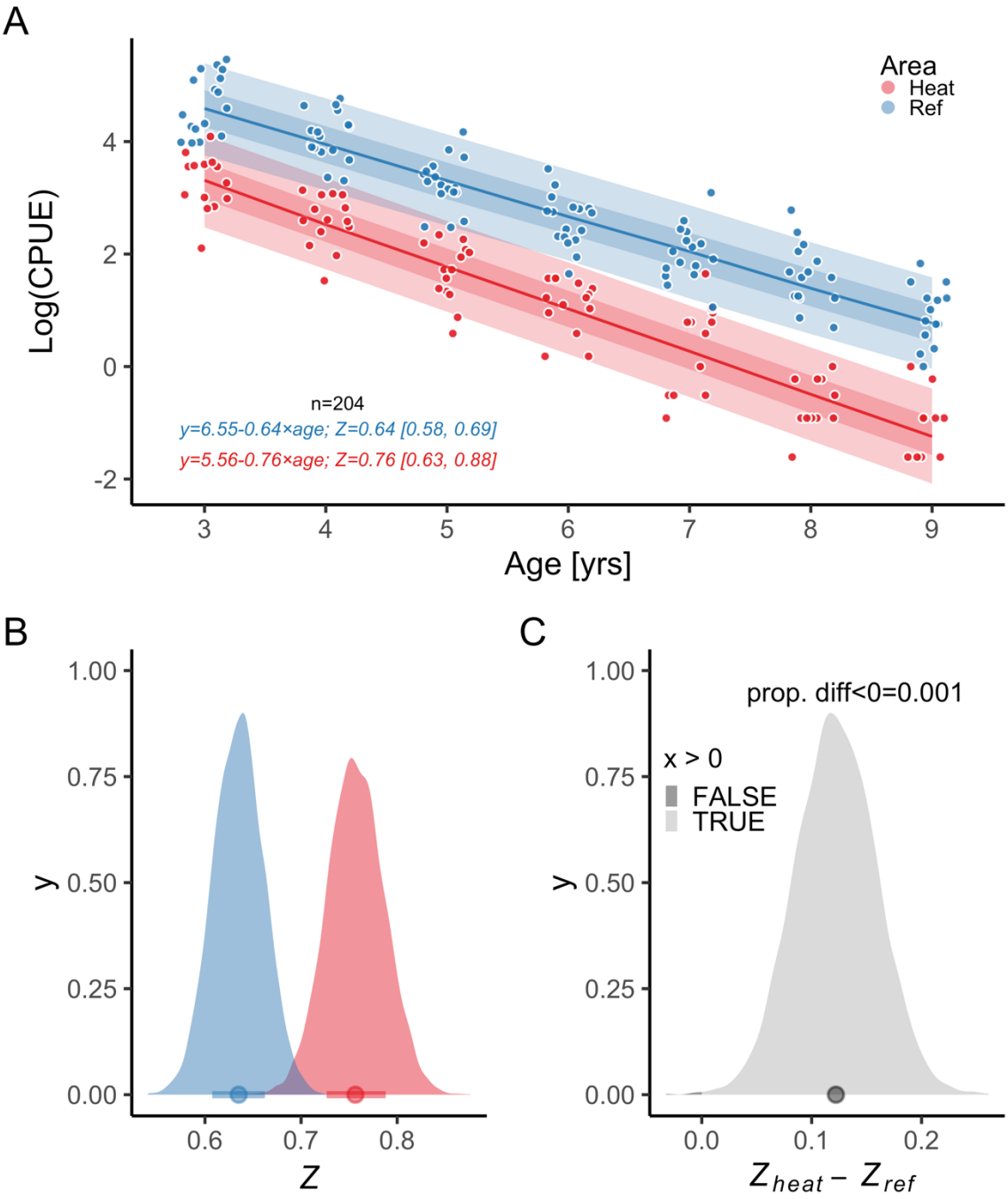

521

522 **Fig. 4.** The instantaneous mortality rate (Z) is higher in the heated area (red) than in the
523 reference (blue). Panel (A) shows the $log\ (CPUE)$ as a function of age, where the slope
524 corresponds to the global $-Z$. Lines show the posterior prediction without group-level effects
525 (i.e., cohort) and the shaded areas correspond to the 50% and 90% credible intervals. The
526 equation uses mean parameter estimates. Panel (B) shows the posterior distributions for
527 mortality rate (Z_{heat} and Z_{ref}), and (C) the distribution of their difference.

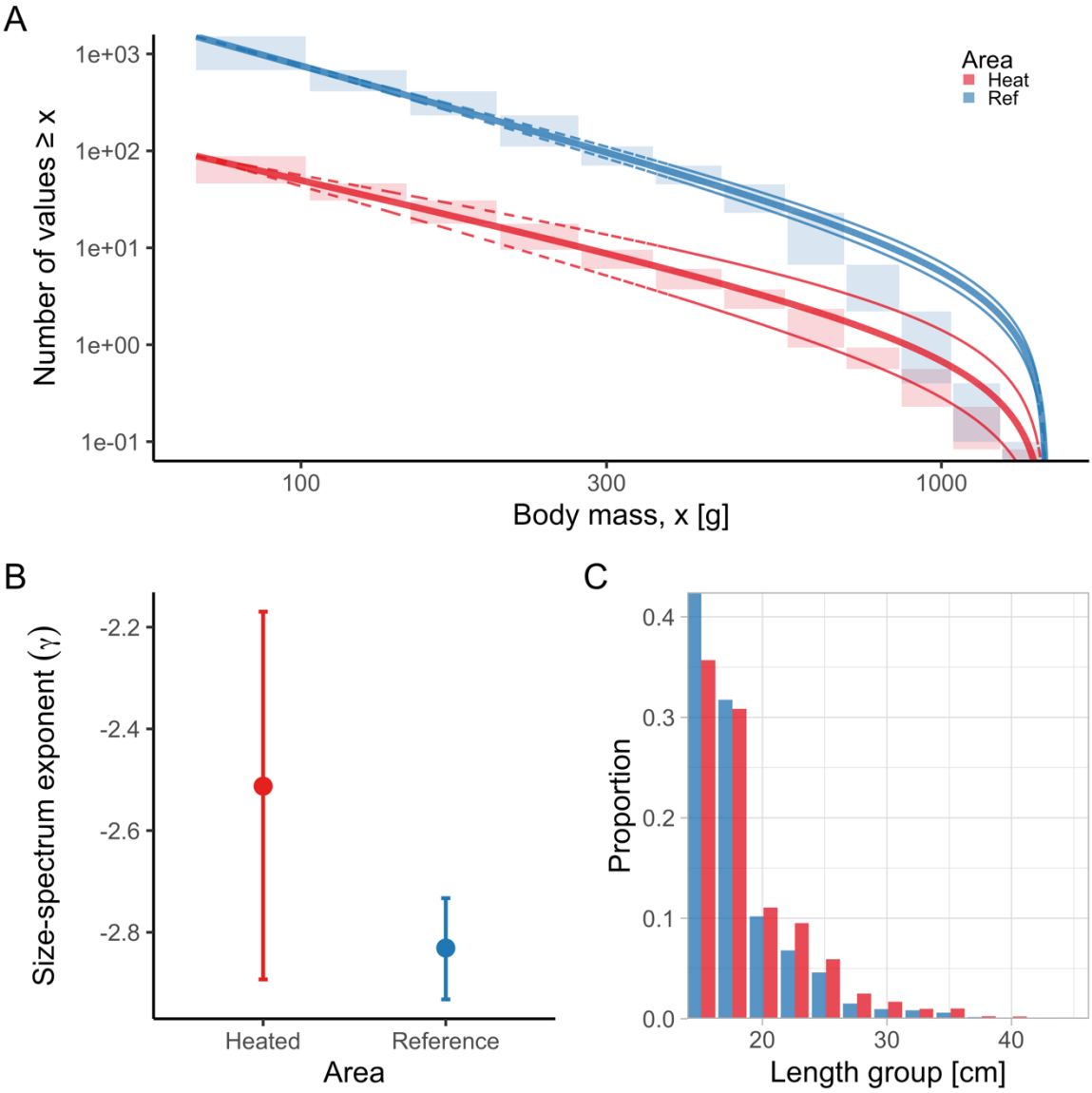

528

529 **Fig. 5.** The heated area (red) has a larger proportion of large fish than the reference area (blue),
530 illustrated both in terms of the biomass size-spectrum (A-B), and histograms of proportions
531 (C). Panel (A) shows the size distribution and MLEbins fit (red and blue solid curve for the
532 heated and reference area, respectively) with 95% confidence intervals indicated by dashed
533 lines. The vertical span of rectangles illustrates the possible range of the number of individuals
534 with body mass ≥ the body mass of individuals in that bin. Panel (B) shows the estimate of the
535 size-spectrum exponent, γ, and vertical lines depict the 95% confidence interval. Panel (C)
536 illustrates histograms of length groups in the heated and reference area as proportions (for all
537 years pooled).